Tran, D.X., Schon, N., Dominati, E., Mackay, A. APPLYING ADVANCED GEOSPATIAL TECHNOLOGIES TO CAPTURE VARIATION IN SOIL HEALTH VARIABLES IN HILL COUNTRY LANDSCAPES. In: *Diverse Solutions for Efficient Land, Water and Nutrient Use.* (Eds C.L. Christensen, D.J. Horne and R. Singh). http://flrc.massey.ac.nz/publications.html. Occasional Report No. 35. Farmed Landscapes Research Centre, Massey University, Palmerston North, New Zealand. 11 pages.

# APPLYING ADVANCED GEOSPATIAL TECHNOLOGIES TO CAPTURE VARIATION IN SOIL HEALTH VARIABLES IN HILL COUNTRY LANDSCAPES

**Duy X. Tran [1*], Nicole Schon [2], Estelle Dominati [1], Alec Mackay [1]**

[1] *AgResearch Grasslands, Palmerston North, New Zealand*

[2] *AgResearch, Lincoln, New Zealand*

[*]Corresponding author: Duy.Tran@agresearch.co.nz

## Abstract

This study aims to quantify the spatial variation in soil health variables in a complex agroecological landscape using modern geospatial analysis tools and technologies. A wide range of soil attributes (soil organic carbon concentration, soil nutrient fertility, bulk density, and earthworm abundance), underlying factors describing the topographical characteristics of the land surface biophysical pattern, along with land use management practices, were utilised to model the spatially explicit pattern of each soil health component. Machine learning techniques were applied to predict soil attributes at a pixel-level across the whole landscape from a limited number of soil samples collected from specific locations. Soil health was quantified using a Composite Soil Health Index (CSHI), calculated from the mean value of the standardized individual soil health indicator which is obtained from the scoring functions for each grid cell. The approach was applied across farmlets that make up the long-term phosphorus (P) fertiliser and sheep grazing experiment at Ballantrae located near Woodville (Southern Hawke's Bay, New Zealand). Results from our study reveal that the variables contributing to soil health varied both across the landscape and between soil health indicators. The study demonstrates that advanced spatial statistical analytics and remote sensing can be effective tools to address the challenge posed by the modelling of biophysical processes in complex agroecological landscapes. Applying such an approach provides a more complete picture on soil health and therefore, can advance the environmental planning and management of farms in New Zealand.

***Key words:*** *Soil attributes, spatially explicit model, hill country, machine learning, farm scale*

## 1. Introduction

Agricultural landscapes with a healthy soil can support sustainable agricultural production and multiple ecosystem services. This in turn strengthens landscape resilience to management pressures, climatic extremes and environmental disturbances (Doran, 2002; Lehmann et al., 2020; Papendick & Parr, 1992). Clearance of native vegetation for agricultural production coupled with agricultural practices on recent, poorly structured soils and shallow soils on medium and steep slopes, has the potential to significantly affect soil health and quality (Alori et al., 2020; Karlen et al., 2003). To protect and where necessary improve soil health, the essential course of action requires an adaptive management strategy, one which can apply the appropriate land use and practices for the targeted areas (Ngo-Mbogba et al., 2015; Safaei et al., 2019; Singh et al., 2014). Mapping soil attributes associated with soil health enables the spatially explicit and detailed information to be quantified, to identify areas where improvement in soil health is needed.

Traditionally, soil health is quantified using in-situ measurement in which soil attributes obtained from soil samples are averaged for the whole study area (Karlen et al., 2019). This provides information for the locations where soil samples were measured, however, is limited in providing a comprehensive pattern of soil health across space. Quantifying spatially explicit patterns of soil health, especially in complex agroecological landscapes, is challenging because soil attributes are heterogenous across space due to the variables in topographies, climate, land cover and land use practices. Often, this complexity cannot be effectively captured by using a limited number of soil samples and applying simple and straight forward models (e.g., interpolation, ordinary least squared regression) (Amirinejad et al., 2011; Svoray et al., 2015).

Recent development in geospatial technologies provides a range of tools, models, and data that enable soil attributes that contributes to soil health to be spatially quantified (Fathololoumi et al., 2020; Padarian et al., 2019; Wadoux et al., 2020). Remote sensing for example provides an array of surface biophysical data which are important soil attributes predictors. Geographical information system (GIS) is a useful tool for the integration of different data sets and types from various sources in a spatial context to identify patterns in soil attributes. Machine learning can analyse large amounts of data and identify patterns and relationships that may not be apparent to the human eye. This can help to improve the accuracy of soil health models. Overall, using machine learning and GIS in modelling soil health can help to improve the accuracy and efficiency of soil health analyses, and provide a more comprehensive understanding of soil health.

This paper sets out to demonstrate how spatially explicit information on soil attributes contributing to soil health in a complex agroecological landscape can be captured using advanced geospatial technologies integrating remote sensing, GIS, and machine learning. The soils from the long-term P fertiliser and sheep grazing experiment located near Woodville were used to test the effectiveness of the approach.

## 2. Research methods

### *2.1. Data and study area*

The soils of the Ballantrae long-term P fertiliser and sheep grazing experiment located near Woodville in southern Hawke's Bay were used as a case study. Three farmlets that have been under different fertiliser management practices include low fertility (LF: 125 kg single superphosphate $ha^{-1}year^{-1}$), high fertility (HF: 375 kg single superphosphate $ha^{-1}year^{-1}$), and no fertility (NF: 0 kg single superphosphate $ha^{-1}year^{-1}$) (Figure 1). Annual mean stocking rates were 6.0, 10.6, and 16.1 SU $ha^{-1}$ for the NF, LF, and HF farmlets, respectively. See Mackay et al. (2021) for detailed description of the study area. A total of 47 soil samples measuring nine soil attributes (Table 1) were used for model training and validation. A further 17 samples that were not used in the modelling stage, were utilised to independently assess the prediction performance.

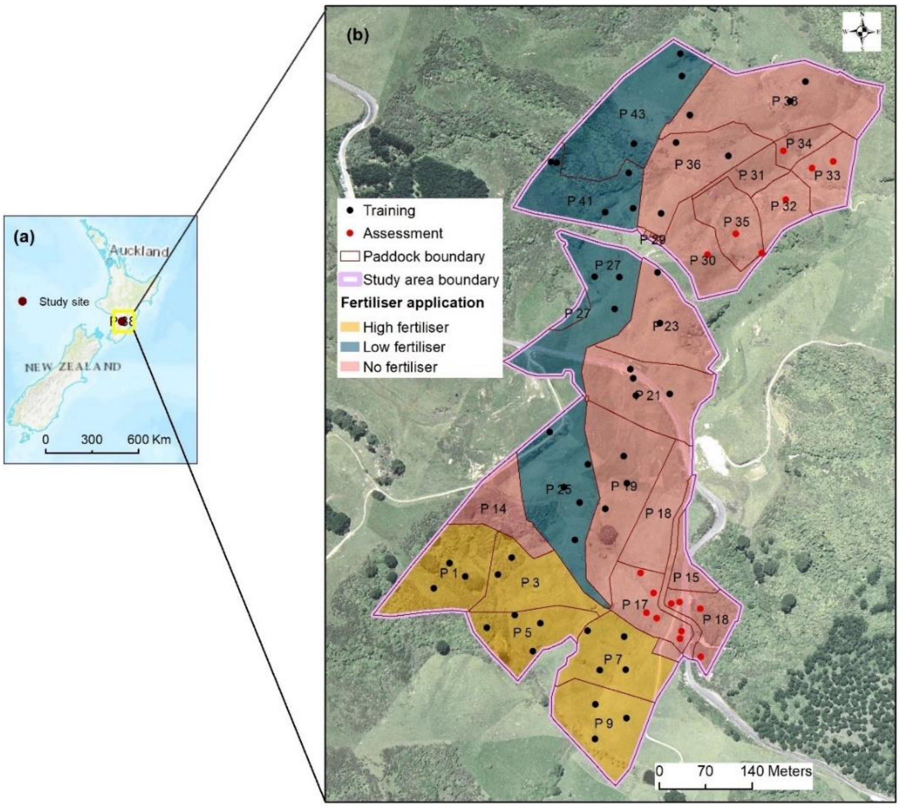


Figure 1: Location of the study area (a), soil attributes sampling sites and three farmlets presenting different fertiliser management practices (b).

Soil attributes predictors (i.e., explanatory variables) cover factors describing the underlying topographical characteristics, land surface biophysical information, and soils and land use management practices. Topographical variables include slope, elevation, aspect, solar radiation, topographical wetness, and roughness. These predictors were calculated from 1m LiDAR-derived Digital Elevation Model (DEM) acquired from the Ballantrae dataset from the long-term experiment. Surface biophysical data variables derived from Sentinel 2 data were normalized difference vegetation index, soil moisture index, bare soil index, normalized difference tillage index, and clay minerals ratio.

Table 1: Soil attributes and descriptive statistics from soil samples collected at the Ballantrae Hill Country Research Station.

| **Indicators** | **Units** | **Mean** | **Median** | **Min** | **Max** | **Range** | **Variance** | **Std. dev** |
|---|---|---|---|---|---|---|---|---|
| TC | % | 5.2 | 5.0 | 3.4 | 8.4 | 5.0 | 1.7 | 1.3 |
| TP | mg/kg | 559.9 | 417.0 | 188.0 | 2120.0 | 1932.0 | 164985.6 | 406.2 |
| TN | % | 0.39 | 0.38 | 0.22 | 0.67 | 0.45 | 0.01 | 0.12 |
| $SO_4$ | mg/L | 15.0 | 10.0 | 4.0 | 56.0 | 52.0 | 154.0 | 12.0 |
| Olsen P | mg/L | 24.0 | 6.0 | 0.0 | 147.0 | 147.0 | 1286.0 | 36.0 |
| CEC | cmol+/kg | 10.0 | 10.0 | 5.0 | 27.0 | 22.0 | 16.0 | 4.0 |
| BD | g/cm$^3$ | 1.32 | 1.32 | 1.02 | 1.62 | 0.60 | 0.02 | 0.13 |
| EW | EW/m$^2$ | 398.0 | 217.0 | 0 | 1425 | 1425 | 147762 | 384 |
| pH | mol/L | 5.4 | 5.3 | 5.0 | 5.8 | 0.8 | 0.0 | 0.2 |

*Total soil carbon (TC), total soil phosphorus (TP), total soil nitrogen (TN), sulphate-S ($SO_4$), phosphorus availability (Olsen P), cation exchange capacity (CEC), bulk density (BD), earthworm abundance (EW)*

### *2.2. Spatially explicit soil health modelling*

In this study we utilised different machine learning tools and algorithms to model the spatially explicit pattern of soil attributes used to describe soil health. These are automated machine learning (AutoML), Forest-based Classification and Regression (FCR), and Empirical Bayesian Kriging (EBK) Regression Prediction. AutoML is a machine learning tool that allows the model training and prediction to be automatically implemented. This tool employs and optimises several algorithms (i.e., Decision Tree, Linear regression, XgBoost, Light GBM, Random Forest, Extra Trees, and Ensemble) to find the best prediction option (Giner, 2022). The FCR tool trains a model based on known values provided as part of a training dataset. This prediction model can then be used to predict unknown values in a prediction dataset that has the same associated explanatory variables. The tool creates models and generates predictions using an adaptation of the random forest algorithm, which is a supervised machine learning method developed by Leo Breiman and Adele Cutler (Breiman, 1996; Cutler et al., 2012). The tool creates many decision trees, called an ensemble or a forest, that are used for prediction. EBK Regression Prediction is a geostatistical interpolation method that uses Empirical Bayesian Kriging (EBK) with explanatory variable rasters (i.e., continuous surfaces, discrete information) that are known to affect the value of the data being interpolated (Bennett, 2018). This approach combines kriging with regression analysis to make predictions that are more accurate than either regression or kriging can achieve on their own. Performance assessment was carried out to evaluate the model's outcomes and results obtained from the most effective model was used for further analysis.

### *2.3. Composite Soil Health Index*

The soil indicators that contribute to soil health were standardised (i.e., rescaled) into a scoring scale (from 0-100) by applying the Gaussian transformation function. The Gaussian function transforms the input values using a normal distribution. The distribution of each of the soil variables was assessed based on a Gaussian distribution function (Moebius-Clune et al., 2011). Scores were developed from cumulative normal distribution (CND) functions as in:

$$p = f(x, \mu, \sigma) = \frac{1}{\sigma\sqrt{2\pi}} \int_{-\infty}^{+\infty} e^{-\frac{1}{2}\left(\frac{x-\mu}{\sigma}\right)^2}$$

where $p$ is the probability (between 0 and 1) that a single observation will fall at a given position in the interval ($+\infty$, $-\infty$), $\mu$ is the mean and $\sigma$ is the standard deviation of the variable. Thresholds for soil variables were determined based on target values published in the literature [Olsen P (Monaghan & Roberts, 2003; Taylor et al., 2016); cation exchange capacity (Drewry et al., 2017); SOC, total soil N, bulk density (Sparling et al., 2008); and earthworm abundance (Schon et al., 2020)]. When absolute thresholds were not established, the target threshold was estimated using local condition (i.e., the max, min, and mean value of soil indicator in the study area).

To normalize the score to the 0 to 100 range, the CND was multiplied by 100, where larger scores are considered to signify better soil functioning. Outputs from this step are nine raster layers measured in the same scale representing each layer of each soil indicator. The "composite soil health index" was computed as the mean value of nine soil attributes layers:

$$CSHI = \frac{\sum p_{1,\ldots n}}{n}$$

Where $p$ is the standardized soil health indicator (i.e., the CND functions), $n$ is the number of soil health indicators contributing to soil health ($n = 9$ in this study). The CSHI used in this study was constructed to just demonstrate how soil attributes contributing to health could be pulled together.

## 3. Results and Discussion

### *3.1. Prediction performance among machine learning techniques*

Table 2 summaries statistical information on the prediction of nine soil attributes including the $R^2$ and prediction error (i.e., root mean squared error; RMSE) obtained from different machine learning algorithms. This provides the model evaluation results for both training and test datasets. The predicted $R^2$ values ranged from 0.45 to 0.97 for training data, and from 0.05 to 0.8 for the independent assessment data.

Table 2: Soil attributes prediction performance using different machine learning techniques for (a) model set, (b) independent assessment set.

| **Indicators** | **Units** | **Auto ML** | | **FCR** | | **EBK Regression** | |
|---|---|---|---|---|---|---|---|
| | | *$R^2$* | *RMSE* | *$R^2$* | *RMSE* | *$R^2$* | *RMSE* |
| ***(a) Model set*** | | | | | | | |
| TC | % | 0.76 | 0.66 | 0.78 | 0.43 | 0.74 | 0.53 |
| TP | mg/kg | 0.93 | 84.35 | 0.80 | 140.05 | 0.93 | 86.87 |
| TN | % | 0.77 | 0.033 | 0.77 | 0.038 | 0.78 | 0.05 |
| $SO_4$ | mg/L | 0.02 | 4.79 | 0.51 | 3.52 | 0.72 | 4.19 |
| Olsen P | mg/L | 0.15 | 25.59 | 0.79 | 11.53 | 0.94 | 7.05 |
| CEC | cmol+/kg | 0.70 | 2.40 | 0.57 | 1.72 | 0.97 | 0.63 |
| BD | $g/cm^3$ | 0.75 | 0.040 | 0.71 | 0.042 | 0.73 | 0.057 |
| EW | $EW/m^2$ | 0.56 | 158 | 0.53 | 186 | 0.69 | 122 |
| pH | mol/L | - | - | 0.60 | 0.05 | 0.45 | 0.087 |
| ***(b) Independent evaluation set*** | | | | | | | |
| TC | % | 0.62 | 0.75 | 0.56 | 0.47 | 0.57 | 0.87 |
| TP | mg/kg | 0.58 | 181.94 | 0.39 | 57.30 | 0.55 | 198.14 |
| TN | % | 0.71 | 0.041 | 0.60 | 0.048 | 0.61 | 0.08 |
| $SO_4$ | mg/L | 0.16 | 2.84 | 0.05 | 3.5 | 0.49 | 3.58 |
| Olsen P* | mg/L | n/a | n/a | n/a | n/a | n/a | n/a |
| CEC | cmol+/kg | 0.80 | 1.60 | 0.10 | 1.32 | 0.35 | 2.32 |
| BD | $g/cm^3$ | 0.44 | 0.081 | 0.57 | 0.047 | 0.40 | 0.133 |
| EW* | $EW/m^2$ | n/a | n/a | n/a | n/a | n/a | n/a |
| pH | mol/L | - | - | 0.02 | 0.06 | 0.034 | 0.182 |

* *Not available due to missing samples.*

Among machine learning methods used in this study, Auto ML was found to be better than others in the prediction performance of TC, TP, TN, and CEC, with a good $R^2$ and RMSE values for both training and test datasets. EBK Regression obtained very high prediction performance for training data, however, this decreased significantly in test data. The FCR method was better than others in the prediction of soil pH and BD. These results suggested that a range of different machine learning methods are required for mapping soil attributes in complex hill country landscapes. This ensures that more accurate and spatially explicit soil attributes are achieved and therefore, provides better information for mapping soil attributes contributing to soil health and their subsequent evaluation.

### *3.2. Spatially explicit pattern of soil attributes*

Results from the model performance assessment were used to produce a set of soil attributes maps for the study area (Figure 2). Soil pH showed a low variation so is not presented. The map (Figure 2a) shows high SOC concentration levels in the west, southeast, and southwest of the southern paddocks. Whereas the northern, central south, and the south areas of the study site had low SOC concentration. It also demonstrated that SOC variation within a paddock could be significantly high, showing that a single paddock may have different levels of SOC concentration. A similar pattern to SOC content was found in the distribution of total N (Figure 2c) and earthworm abundance (Figure 2h), whereas soil bulk density (Figure 2g) presented an inverse pattern compared to these attributes.

The pattern of total P (Figure 2b) demonstrated very high values in the south and low values in the north of the farm while low to medium values were seen in the centre, reflecting the different P fertiliser histories. Olsen P and Sulphate-S patterns in the south end paddocks were relatively aligned with that of total P distribution. It is noted that the Olsen P pattern showed very low values in the eastern part, extremely high values in the southern part, and relatively low values in the remaining area of the study site. This pattern is closely aligned with the fertiliser management practices applied in the study area.

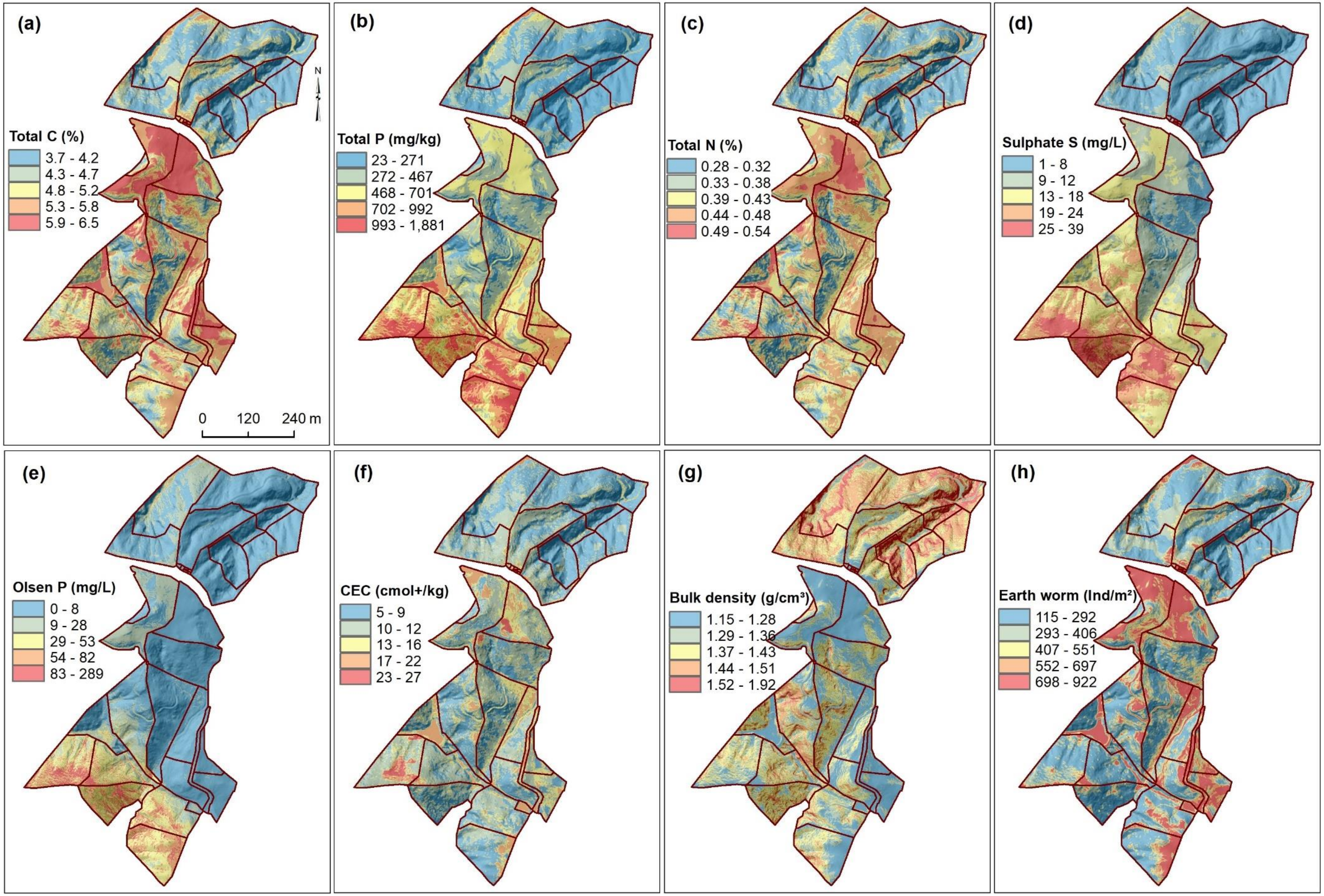


Figure 2: Maps of predicted soil attributes in the study area: (a) Total C (%), (b) Total Phosphorus (mg/kg), (c) Total Nitrogen, (d) Sulphate-S (mg/L), (e) Olsen P (mg/L), (f) Cation exchange capacity (cmol+/kg), (g) Soil bulk density, and (h) Earthworm abundance (Ind./$m^2$).

The functions for selected soil attributes in the study area obtained using the CND function are presented in Figure 3. The horizontal axis within each graph shows absolute values of each individual soil attribute. The vertical axis represents equivalent standardised scores. Olsen P, total P, and Sulphate-S had similar shaped curves. The shape of soil functions for these indicators shows that the midpoint of the normal distribution obtained the highest score, and standardised scores decrease as values of the soil attributes move from the midpoint until reaching the least preference values. Earthworm abundance, total N, total C, cation exchange capacity, and soil pH showed a similar scoring function. The shape of the scoring function for these attributes demonstrates that soil attributes achieve the highest score when their absolute measurements are greater than the target values. Bulk density presented an opposite scoring function in comparison to these soil attributes. It is important to noted that the shapes and distributions of soil functions presented here are specific for the soils in the study area, it may vary dependent on different target values and across study areas.

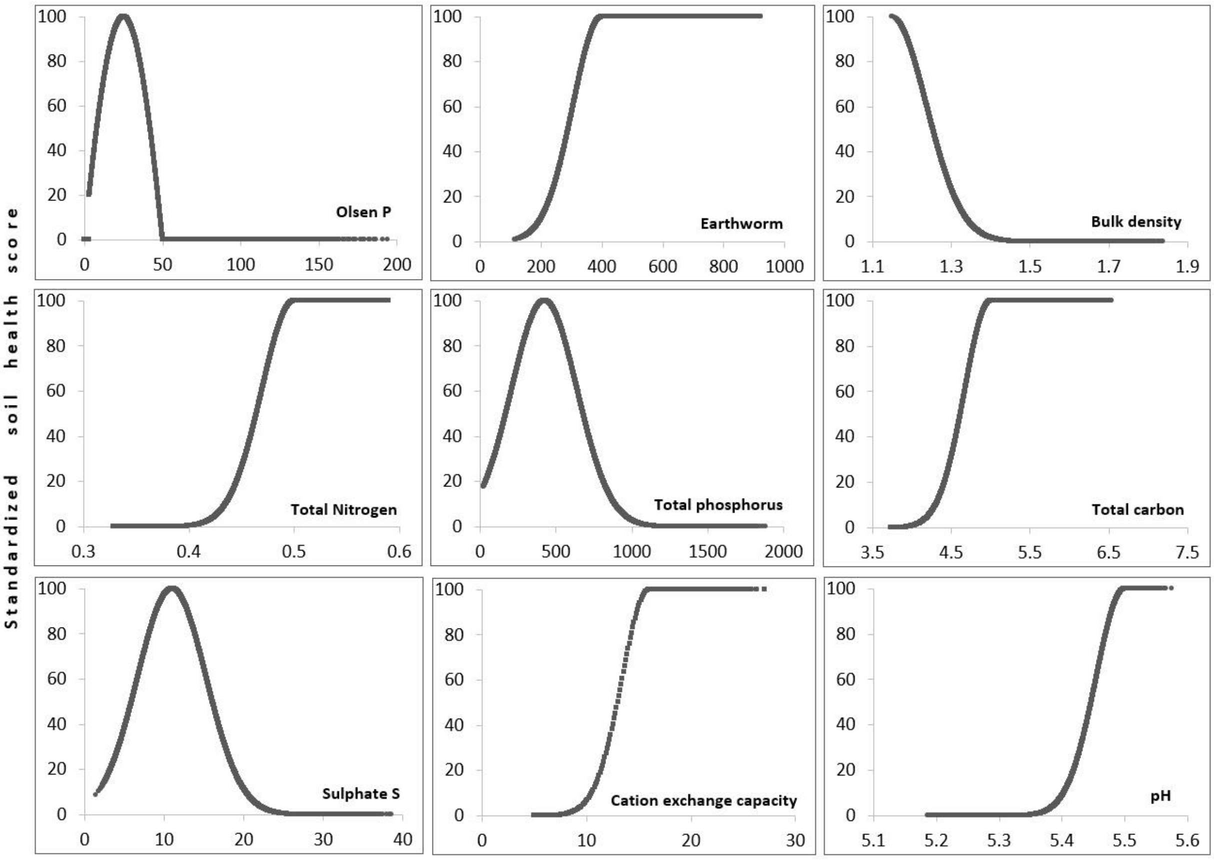


Figure 3: Cumulative normal distribution functions for the relationship between a change in the soil attribute contributing to soil health and its contribution to the standardised soil health score.

### *3.3. Spatial variation in soil attributes contributing to soil health*

The spatially explicit CSHI pattern for the study area is presented in Figure 4. Both heterogenous and homogenous patterns of CSHI were found in the study area. High CSHI (score > 70) accounted for only 3.6% of the total land area. Moderate CSHI (50 < CSHI ≤ 70) occupied 26% and were mainly concentrated in the flat paddocks (e.g., LF farmlet (P27), NF farmlet (P23, P15, P18)) located in the central north area and southeast of the study site. Low and very low CSHI values were dominant classes (80% of the study area's land) and distributed in the north (NF farmlet) and southwest areas (HF farmlet). It is also seen that the CSHI values were variable between paddocks. For example, mean CSHI values by paddock in Figure 4 revealed a significant contrast between paddocks. For instance, CSHI values were four times greater in the highest paddock (P27) than in the lowest paddock (P33). The CSHI values also varied within a single paddock. For instance, both highest and lowest CSHI values were observed in some paddocks (e.g., P21, P19, P25). The CSHI values were closely aligned with the pattern of topography, showing that high values often appeared on flat areas (i.e., low slope) such as hilltops and valley floors whereas steepland areas (i.e., slopes > 25$^{o}$) tended to have lower CSHI values.

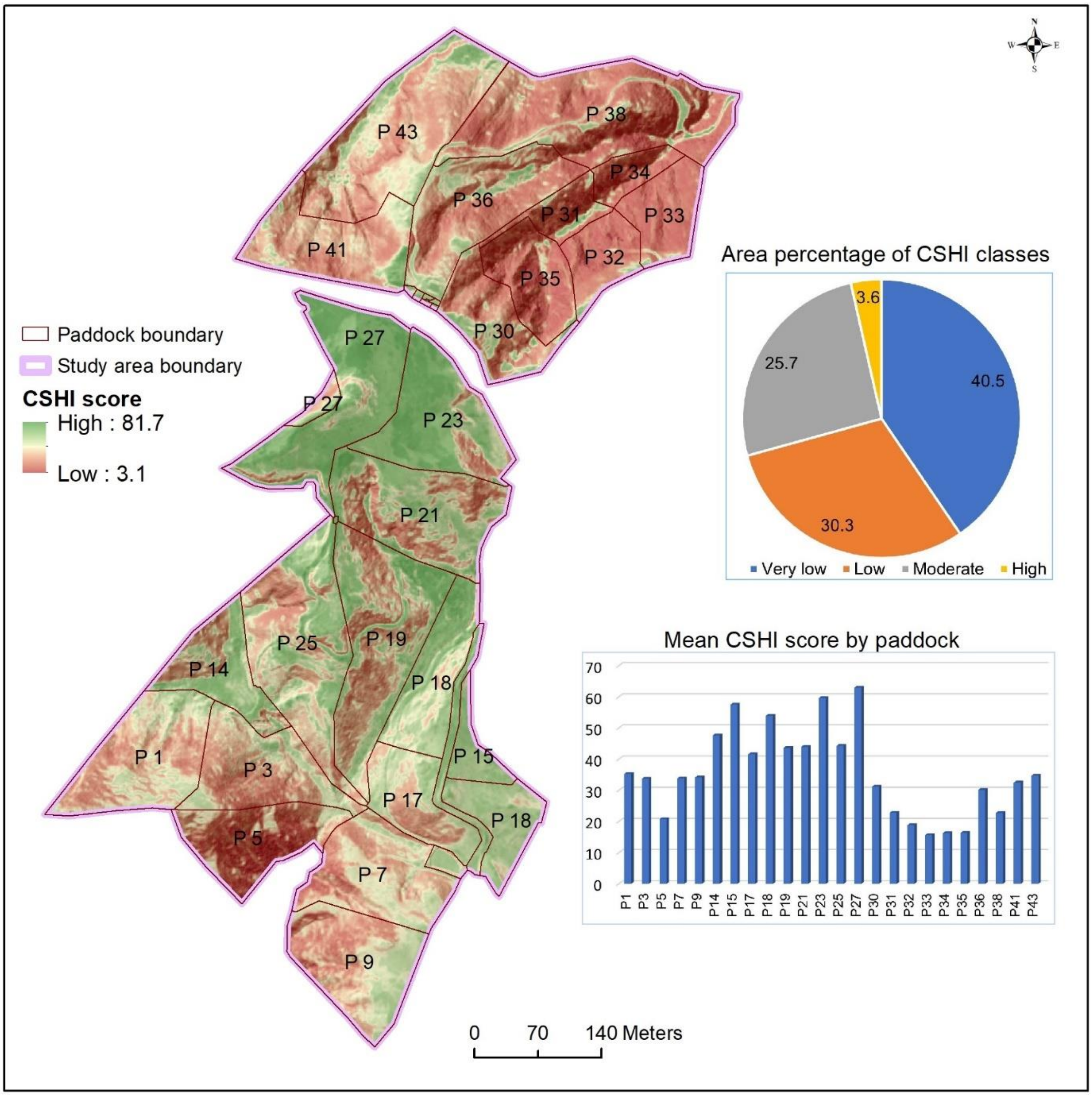


Figure 4: Composite Soil Health Index values across the study area (a). The area percentage chart is classified into 5 levels: high (score > 70, moderate (50 < overall score ≤ 70), low (30 < overall score ≤ 50), very low (overall score < 30).

The radar plots (Figure 5) demonstrate the contribution of different soil attributes to soil health by paddock under different P fertilization regimes and grazing management. Highly fertilised paddocks (P1-P9, orange) had low and very low CSHI values. This is because these paddocks had very low scores in Sulphate-S, total P, and bulk density. Different CSHI values were found in LF and NF paddocks, indicating that soil health is not only impacted by land management but also dependent on landscape patterns (e.g., topography and soils).

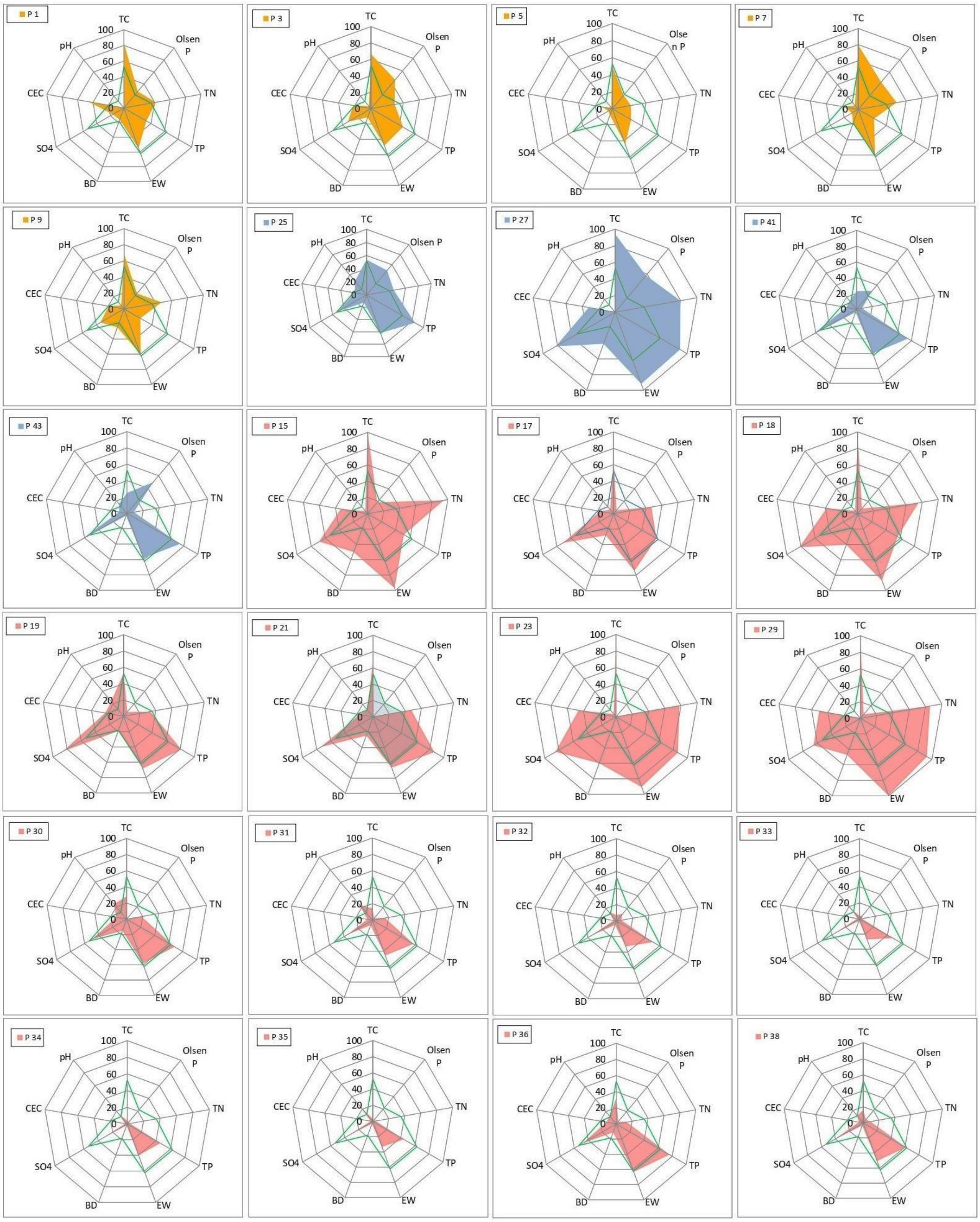


Figure 5: Predicted soil attributes contributing to soil health in the study area by paddock across the high fertilised paddocks (orange), low fertilised paddocks (blue), no fertilised paddocks (red). The green line presents mean CSHI value for the farm. Total C (TC), Total Phosphorus (TP), Total Nitrogen (TN), Earthworm abundance (EW), Soil bulk density (BD), Sulphate-S ($SO_4$), Cation exchange capacity (CEC), and soil pH (pH).

### *3.4. Implications for soil health mapping and management practices*

Studying soil health in the hill country of New Zealand presents several challenges, including the complexity and heterogeneity of the soils and topographies, and often limited number of soil sample sites. As such, it is difficult to obtain an understanding of the variation that is found in the soil attributes that contribute to soil health and how they change across the landscape from the influence of management practices. To overcome this limitation, we applied an approach that integrated remote sensing, GIS, and machine learning to model the spatially explicit soil attributes that contribute to soil health where there was only a limited number of soil samples. Our study demonstrated that using this integrated modelling approach provides a more complete picture of the changes that occur in soil attributes that contribute to soil health. This approach provides vital information for farmers/land managers to help them identify areas to focus on and define relevant management practices. Geospatial models such as this one can help precision decision making and therefore minimise management costs and maximise the positive impacts of soil management on farm. Work is ongoing to 1) analyse the relationship between soil attributes pattern and underlying environment and management factors, 2) explore which soil attributes may be most informative for soil health in a geospatial context, and therefore the most important to manage for farmers 3) how scoring functions can better represent soil health targets, and 4) how to maintain soil attribute level detail that is hidden within a composite soil health score.

## 5. Conclusions

Advanced remote sensing, GIS, and statistical methods can facilitate the mapping of soil health, which is critical for sustaining production and efficient environmental management. These tools can effectively map the spatially explicit pattern of the soil attributes that contribute to soil health and show variations between and within paddocks. Soil health is influenced by various factors, including topographical patterns, surface biophysical features, soil types, and management practices. Work is ongoing to refine this approach further. Mapping soil attributes contributing to soil health at the farm scale provides vital information that can inform sustainable environmental management practices. The use of these advanced techniques allows farmers and land managers to gain a better understanding of the distribution of soil health across their land, enabling them to make informed decisions about land use and management practices that can lead to more efficient and sustainable agricultural practices.


## Acknowledgements

We would like to thank the technical staff in the Land Use Function and Evaluation team for collecting and processing the soil samples data. This study was supported by the AgResearch SSIF programme NZ Bioeconomy in the Digital Age (NZBIDA).


## References


Alori, E. T., Adekiya, A. O., & Adegbite, K. A. (2020). Impact of agricultural practices on soil health. *Soil Health,* 89-98.

Amirinejad, A. A., Kamble, K., Aggarwal, P., Chakraborty, D., Pradhan, S., & Mittal, R. B. (2011). Assessment and mapping of spatial variation of soil physical health in a farm. *Geoderma, 160*(3-4), 292-303.

Bennett, L. (2018). Machine learning in ArcGIS. *ArcUser, 21*, 8-9.

Breiman, L. (1996). Bagging predictors. *Machine learning, 24*, 123-140.

Cutler, A., Cutler, D. R., & Stevens, J. R. (2012). Random forests. *Ensemble machine learning: Methods and applications*, 157-175.

Doran, J. W. (2002). Soil health and global sustainability: translating science into practice. *Agriculture, ecosystems & environment, 88*(2), 119-127.

Drewry, J., Parkes, R., & Taylor, M. (2017). Soil quality and trace elements for land uses in the Wellington region and implications for farm management. *Science and policy: Nutrient management challenges for the next generation*.

Fathololoumi, S., Vaezi, A. R., Alavipanah, S. K., Ghorbani, A., Saurette, D., & Biswas, A. (2020). Improved digital soil mapping with multitemporal remotely sensed satellite data fusion: A case study in Iran. *Science of the Total Environment, 721*, 137703.

Giner, N. (2022). *AutoML in ArcGIS Pro 3.0*. Retrieved 28th February from https://www.esri.com/arcgis-blog/products/arcgis-pro/analytics/automl-in-arcgis-pro-3-0/

Karlen, D. L., Ditzler, C. A., & Andrews, S. S. (2003). Soil quality: why and how? *Geoderma, 114*(3-4), 145-156.

Karlen, D. L., Veum, K. S., Sudduth, K. A., Obrycki, J. F., & Nunes, M. R. (2019). Soil health assessment: Past accomplishments, current activities, and future opportunities. *Soil and tillage research, 195*, 104365.

Lehmann, J., Bossio, D. A., Kögel-Knabner, I., & Rillig, M. C. (2020). The concept and future prospects of soil health. *Nature Reviews Earth & Environment, 1*(10), 544-553.

Mackay, A. D., Vibart, R., McKenzie, C., Costall, D., Bilotto, F., & Kelliher, F. M. (2021). Soil organic carbon stocks in hill country pastures under contrasting phosphorus fertiliser and sheep stocking regimes, and topographical features. *Agricultural Systems, 186*, 102980.

Moebius-Clune, B., Idowu, O., Schindelbeck, R., Van Es, H., Wolfe, D., Abawi, G., & Gugino, B. (2011). Developing standard protocols for soil quality monitoring and assessment. Innovations as key to the green revolution in Africa: exploring the scientific facts,

Monaghan, J. M. R. M. R., & Roberts, A. (2003). Balancing phosphorus requirements for milk production and water quality. Proceedings of the New Zealand Grassland Association,

Ngo-Mbogba, M., Yemefack, M., & Nyeck, B. (2015). Assessing soil quality under different land cover types within shifting agriculture in South Cameroon. *Soil and tillage research, 150*, 124-131.

Padarian, J., Minasny, B., & McBratney, A. B. (2019). Using deep learning for digital soil mapping. *Soil, 5*(1), 79-89.

Papendick, R. I., & Parr, J. F. (1992). Soil quality—the key to a sustainable agriculture. *American Journal of Alternative Agriculture, 7*(1-2), 2-3.

Safaei, M., Bashari, H., Mosaddeghi, M. R., & Jafari, R. (2019). Assessing the impacts of land use and land cover changes on soil functions using landscape function analysis and soil quality indicators in semi-arid natural ecosystems. *Catena, 177*, 260-271.

Singh, A., Bordoloi, L., Kumar, M., Hazarika, S., & Parmar, B. (2014). Land use impact on soil quality in eastern Himalayan region of India. *Environmental monitoring and assessment, 186*, 2013-2024.

Svoray, T., Hassid, I., Atkinson, P. M., Moebius-Clune, B. N., & Van Es, H. M. (2015). Mapping soil health over large agriculturally important areas. *Soil Science Society of America Journal, 79*(5), 1420-1434.

Taylor, M., Drewry, J., Curran-Cournane, F., Pearson, L., McDowell, R., & Lynch, B. (2016). Soil quality targets for Olsen P for the protection of environmental values. *Integrated Nutrient and Water Management for Sustainable Farming, Massey University, Palmerston North, New Zealand*.

Wadoux, A. M.-C., Minasny, B., & McBratney, A. B. (2020). Machine learning for digital soil mapping: Applications, challenges and suggested solutions. *Earth-Science Reviews, 210*, 103359.